IX CONGRESSO BRASILEIRO DE ENGENHARIA E CIÊNCIAS TÉRMICAS
9th BRAZILIAN CONGRESS OF THERMAL ENGINEERING AND SCIENCES

Paper CIT02-0323

AN A POSTERIORI ERROR ESTIMATE FOR FINITE VOLUME METHODS: PARABOLIC PROBLEMS

Marcio Arêdes Martins
Departamento de Engenharia Mecânica - UFMG - Av. Antônio Carlos, 6627 - 31270-901 - Belo Horizonte - MG - Brazil
aredes@demec.ufmg.br

Leandro Soares Oliveira
Departamento de Engenharia Química - UFMG - Rua Espírito Santo, 35, 6º andar - 31160-030 - Belo Horizonte - MG - Brazil
leandro@deq.ufmg.br

Denise Burgarelli
Departamento de Matemática - ICEX/UFMG - Av. Antônio Carlos, 6627 - 31270-901 - Belo Horizonte - MG - Brazil
burgarel@mat.ufmg.br

Ramón Molina Valle
Departamento de Engenharia Mecânica - UFMG - Av. Antônio Carlos, 6627 - 31270-901 - Belo Horizonte - MG - Brazil
ramon@vesper.demec.ufmg.br

Abstract. *An a posteriori error estimate for finite volume methods in triangular meshes is developed and successfully implemented for parabolic heat transfer problems. The proposed error estimate belongs to the class of truncation-error estimates. A polynomial function was successfully employed in the estimation of the solution used in the error formulation. A simple and reliable h-type adaptive methodology was also developed and successfully implemented. The major feature of the adaptive methodology consists on the fact that the proposed error estimate does not require the solution of systems of equations as in the case of estimates belonging to other classes. The error differences using analytical and estimate solutions were compared for three parabolic heat transfer problems, and a good performance of the adaptive procedure was verified.*

Keywords. *unstructured triangular meshes; adaptive refinement; heat transfer.*

1. Introduction

The finite volume is a discrete numerical method suitable for the solution of conservation laws described by means of elliptic, parabolic or hyperbolic partial differential equations. This method has been extensively used in several engineering fields, mainly in computational fluid dynamics (Frink, 1994; Haselbacher et all, 1999). Two important features of the finite volume method are the use of arbitrary control volume geometries that leads to robust schemes, and the local conservation of the numerical fluxes between each pair of neighboring control volumes. This last feature makes the method attractive in simulation problems where the flux is of relevance, such as problems of fluid mechanics, heat and mass transfer.

The convergence theory of the finite volume method in several space dimensions has only recently been undertaken. As a result of such theory, the complete discrete spaces and the respective norms are known, so error estimates can be now formulated. A mathematical framework of the finite volume method is presented and thoroughly discussed by Herbin (1995) and Galouet and Herbin (1996).

Methodologies for error estimation and mesh adaptation have been proposed in order to improve the accuracy of numerical solution of partial differential equations. A way to reduce the numerical error is by reducing the characteristic size of the mesh polyhedrals, and the resulting procedure is called adaptive h-refinement. There are only a few methodologies in the literature (Berger and Collela, 1989; Ilinca et all, 1995; Zhang et all, 2000, Ilinca et all, 2000) for the finite volume method and this late development can be justified by a previous lack of mathematical support, which is required for developing the error estimate formulations. Researchers have used finite element tools to formulate error indicators (Baranger et all, 1996; Arbogast et all, 1997) for finite volume methods. However, the results were not completely accepted by the finite-volume community. The non-acceptance was based on the fact that the finite volume is a discrete method, in which the dependent variables are defined by a single discrete location into the mesh polyhedral (usually the centroid), whereas in the finite element method, the dependent variables are defined by a combination of continuous test functions. Thus, the approximate solutions in finite volume methods are formulated using a set of piecewise constant functions and, therefore, the respective norms used to measure the numerical error are discrete norms.

In the finite volume error estimate framework, Richardson extrapolation is the most popular methodology and it has been used to solve adaptively a few engineering problems (Ilinca et all, 2000; Baranger et all, 1996; Arbogast et all, 1997; Thompson and Ferziger; 1989). This estimate is quite reliable on refined meshes, since it takes into account the smoothness of the spatial variation. However, the method requires the solutions on at least two meshes, differing in size by a factor of two, just to estimate the error throughout the computational domain. An error estimate based on solution reconstruction using a weighted least-square interpolation scheme was also proposed in the literature (Ilinca et all, 1995). This estimate reconstructs the solution by means of piecewise linear or quadratic functions, used to calculate the derivatives at the discrete points. Although this estimate was inherently simple, it was verified in (Zhang et all, 2000, Ilinca et all, 2000) that it was less effective than the others when strong nonlinearities were present, so it was suitable only to solve problems where suitably refined initial meshes can be generated and smooth solutions are present. A third class of error estimate presented in the literature was based on an error equation, which was derived from the original system of equation. In this estimate, error source terms were obtained by an analysis of the numerical scheme. This error estimate technique was compared to the previous one in (Klopfer and McRae, 1983; Zhang et all, 2000, Ilinca et all, 2000) where good effectiveness of estimate could be verified. Again, this last error estimate requires the solution of a system of equations and its formulation leads to a specific equation for the error, which is fully dependent on the primary problem equations. Further details on this error estimate technique can be found in (Klopfer and McRae, 1983; Zhang et all, 2000, Ilinca et all, 2000).

Based on the presented review, it is clearly noticeable that most of the error estimation procedures for finite volume methods require the solution of a system of equations. As a conclusion, an expressive computational effort is necessary to solve the problem adaptively. In the present work, an *a posteriori* error estimate, based on local solution reconstruction, that can be expressed as an algebraic equation is proposed. Hence, the need for solutions of systems of equations in the error estimation procedure is eliminated. The proposed estimate can be classified as a truncation-error type. As previously discussed, the main objective consists on the development of a fast and reliable *a posteriori* error estimate and an adaptive procedure for finite volume methods on unstructured triangular meshes.

The paper is organized as follows. Section 2 describes a finite volume discretization scheme for triangular meshes. The error estimate and the adaptive procedure are presented in Section 3. In the last section, a study of the performance of the proposed adaptive solution are presented for three generic parabolic heat transfer problems.

2. Finite volume discretization scheme

Consider the generic parabolic problem:

$$\frac{\partial u(\mathbf{x},t)}{\partial t} + \nabla \cdot \left(- k(\mathbf{x}) \nabla u(\mathbf{x},t)\right) = f(\mathbf{x},t) \qquad \text{in } \Omega \tag{1a}$$

$$u(\mathbf{x},0) = u_0(\mathbf{x}) \qquad \text{in } \Omega \tag{1b}$$

$$u(\mathbf{x},t) = u_p(\mathbf{x},t) \qquad \text{in } \partial\Omega \tag{1c}$$

$$- k(\mathbf{x}) \nabla u(\mathbf{x},t) \cdot \mathbf{n} = g(\mathbf{x},t) \qquad \text{in } \partial\Omega \tag{1d}$$

$$- k(\mathbf{x}) \nabla u(\mathbf{x},t) \cdot \mathbf{n} = h(\mathbf{x},t)\left(u(\mathbf{x},t) - u_\infty\right) \qquad \text{in } \partial\Omega \tag{1e}$$

where $u(\mathbf{x}, t)$ is a scalar field (e. g. temperature), $k(\mathbf{x})$, $f(\mathbf{x}, t)$, $g(\mathbf{x}, t)$ and $h(\mathbf{x}, t)$ are functions, $u_0(\mathbf{x})$ is the initial condition, $u_p(\mathbf{x}, t)$ is the scalar field at the boundary $\partial\Omega$ of the domain (Ω), and u_∞ is the scalar value surrounding $\partial\Omega$. Eqs. (1c), (1d) and (1e) represent the boundary conditions of Dirichlet, Neumann and Robin, respectively.

Lets define $\Omega_i \in \Omega$ in which $\Omega = \cup \Omega_i$ as a set of triangular control volumes (i.e. cells). The integral form of Eq. (1a) is given by:

$$\int_{\Omega_i} \frac{\partial u(\mathbf{x},t)}{\partial t} d\mathbf{x} - \int_{\partial\Omega_i} k(\mathbf{x}) \nabla u(\mathbf{x},t) \cdot \mathbf{n} dS = \int_{\Omega_i} f(\mathbf{x},t) d\mathbf{x} \qquad \text{in } \Omega_i \in \Omega \tag{2}$$

In the finite volume discretization scheme, the diffusion flux $-k(\mathbf{x})\nabla u(\mathbf{x}, t)$ on the shared triangular faces needs to be approximated. In order to deal with generic meshes and diffusion matrices, an approximation of the entire gradient should be carried out. Among the methodologies used to approximate the contour integral in Eq. (2) (Frink, 1994; Herbin, 1995; Galouët and Herbin, 1996; Feistauerk et all, 1997; Haselbacher et all, 1999), the diamond cell method it will be used in this work due to the inherent simplicity and existent mathematical framework. Its definition is depicted in Fig. 1, where $\mathbf{x}_i$ and $\mathbf{x}_j$ denote the coordinates of the centroids of two neighbor triangles, $\mathbf{x}_n$ and $\mathbf{x}_s$ are the vertices coordinates such that $|(\mathbf{x}_i - \mathbf{x}_j) \times (\mathbf{x}_n - \mathbf{x}_s)| > 0$, $\mathbf{x}_f$ is the coordinate at the shared face, ξ and η constitute a non-orthogonal basis.

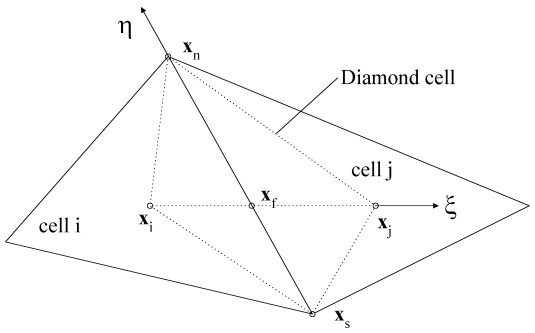

Figure 1. Notation and diamond cell definition for triangular meshes.

Using the diamond cell method and an implicit time integration scheme, Eq. (2) is approximated by means of the discrete gradient at each face belonging to cell i (Fig. 1) resulting in

$$(u_i - u_i^0)\frac{A_i}{\Delta t} - \sum_{j=1}^{3} k(\mathbf{x}_f)\Delta\eta\left[\frac{u_j - u_i}{\Delta\xi(\mathbf{t}_\xi \cdot \mathbf{n}_\eta)} - \frac{u_n - u_s}{\Delta\eta}\left(\frac{\mathbf{t}_\xi \cdot \mathbf{t}_\eta}{\mathbf{t}_\xi \cdot \mathbf{n}_\eta}\right)\right] = f(\mathbf{x}_i, t)A_i \qquad \text{in } \Omega_i \in \Omega \tag{3}$$

where u_i^0 is the discrete scalar at the previous time step, **n** and **t** are the unit normal and the tangential vector at the basis ξ and η, respectively, Δξ and Δη are the distances between neighboring centroids and the nodes n and s at the shared face, respectively, and A_i is the area of the triangular cell Ω_i.

The finite volume discrete form of Eq. (1), given by Eq (3), is attractive for the solution of problems where highly irregular geometries are present. The convergence of the scheme holds even the local basis is not orthogonal. Further details on this subject are given in (Eymard et all, 1997). The nodal values u_n and u_s are approximated by a least-square interpolation scheme, using the centroid of the triangle that share the respective nodes (Frink, 1994; Eymard et all, 1997). Thus, the implicit scheme results in a set of algebraic equations based on the cell centroids only. The application of the boundary conditions given by Eqs. (1c)-(1e) is presented and thoroughly discussed in (Eymard et all, 1997).

3. Error estimate and adaptivity

Whenever a numerical method is used to solve a differential equation, a difference will exist between the numerical and the exact solutions. If the exact solution is known, the error in each mesh cell (i.e. local error), as well as in the whole domain (i.e. global error), can be calculated using several norms. In most engineering problems, an exact solution is not possible to be obtained, and therefore the solution error cannot be calculated. Hence, it should be estimated. When an estimate is used instead of the exact solution, it can be used to control both local and global solution errors. This control is made by means of an adaptive procedure. The most popular adaptive procedures are of the h-type, which are based on establishing a relationship between the size of the mesh cells and the solution error. The procedures usually consist on distributing the global error equally over the mesh, increasing or decreasing the size of the mesh cells as needed.

Lets drop the time reference for u(**x**, t) as u(**x**) for a sake of simplicity. The error e_i for the triangle Ω_i is defined in this work as

$$e_i = u(\mathbf{x}_i) - u_i \tag{4}$$

where u($\mathbf{x}_i$) and u_i are the estimated and the finite volume solutions, respectively, at the centroid of the triangle Ω_i. The norms used to measure the error are usually the L^2 and the H_1 norms (Eymard et all, 1997; Coudière, 1999). The also called energy norm (H_1) is written in the discrete form as:

$$\| e_i \|_{H_1} = \left[\sum_{j=1}^{3} \Delta\xi\Delta\eta\left(\frac{u(\mathbf{x}_i) - u(\mathbf{x}_j)}{\Delta\xi} - \frac{u_i - u_j}{\Delta\xi}\right)^2\right]^{\frac{1}{2}} \tag{5}$$

The choice for an error norm depends on the problem of interest. It is well established in the finite element method community that the energy norm is more suitable to measure the estimate error when elliptic and parabolic problems are solved, since the entire formulation is dependent on the gradient, as also observed in the finite volume discretization scheme. Notice that the continuous form of Eq. (5) consists on a measure of the difference between the gradients of the

numerical and the estimate solutions. Thus, this norm is equivalent to the well known energy norm commonly employed in works dealing with finite element methods (Herbin and Marchand, 2001).

The error estimate proposed in this work belongs to the class of truncation error estimates, which are based on one-dimensional Taylor series. Along the ξ axis (Fig. 1), the solution at any ξ coordinate can be evaluated by:

$$u(\xi) = u_i + \frac{\partial u_i}{\partial \xi}\frac{d_\xi}{1!} + \frac{\partial^2 u_i}{\partial \xi^2}\frac{d_\xi^2}{2!} + \frac{\partial^3 u_i}{\partial \xi^3}\frac{d_\xi^3}{3!} + \cdots + \frac{\partial^n u_i}{\partial \xi^n}\frac{d_\xi^n}{n!} + \cdots \tag{6}$$

where $u(\xi)$ is the solution along ξ, and d_ξ is the distance from $\xi = 0$. Recall that the approximate gradient in Eqs. (3) and (5), between the shared centroids i and j, obey Eq. (6) truncated in the second term, for $\xi = \Delta\xi$ and $u(\Delta\xi) = u_j$, thus

$$\frac{\partial u_i}{\partial \xi} = \frac{\partial u(\mathbf{x}_f)}{\partial \xi} = \frac{u_j - u_i}{\Delta\xi} \tag{7}$$

The estimate consists on an *a posteriori* evaluation of the first four terms of the Taylor series, so a more reliable approximation for $u(\mathbf{x})$ at the cell face can be obtained. The polynomial

$$u(\xi) = \sum_{k=0}^{3} a_k \xi^k \tag{8}$$

consists on a particular solution of Eq. (6) and it satisfies the previous restrictions. The a_k coefficients can be evaluated by

$$\begin{aligned} \xi = 0 \quad &\rightarrow \quad u(\xi) = u_i \\ \xi = 0 \quad &\rightarrow \quad \partial u(\xi)/\partial \xi = \nabla u_i \cdot \mathbf{t}_\xi \\ \xi = \Delta\xi \quad &\rightarrow \quad u(\xi) = u_j \\ \xi = \Delta\xi \quad &\rightarrow \quad \partial u(\xi)/\partial \xi = \nabla u_j \cdot \mathbf{t}_\xi \end{aligned} \tag{9}$$

where ∇u_i and ∇u_j are the gradients at triangles Ω_i and Ω_j, respectively. Using the conditions in Eq. (9), the a_k coefficients could be obtained, so the error norm presented in Eq. (5) can be rewritten as (Eymard et all, 1997; Coudière et all, 1999)

$$\| e_i \|_{H_1} = \left[\sum_{j=1}^{3} \Delta\xi_f \Delta\eta \left(\frac{u(\mathbf{x}_i) - u(\mathbf{x}_f)}{\Delta\xi_f} - \frac{u_i - u_f}{\Delta\xi_f} \right)^2 \right]^{\frac{1}{2}} \tag{10}$$

where u_f and $u(\mathbf{x}_f)$ are the finite volume and the estimate solutions at the shared face between the triangles Ω_i and Ω_j, respectively, and $\Delta\xi_f$ is the distance along the ξ axis between the centroid i and the cell face coordinate $\mathbf{x}_f$.

Different from error estimate techniques based on residuals (Klopfer and McRae, 1983; Thompson and Ferziger, 1989; Arbogast et all, 1997), the proposed formulation not only presents an error estimate (Eq. (10)) but also an estimate for the solution, given by Eq. (8). The discrete gradient required in the error estimate can be evaluated by any three non-collinear known points, using the gradient theorem, as presented by (Frink, 1994; Pan and Cheng, 1993; Arminjon and Madrane, 1999)

In order to obtain an adaptive solution, a methodology in which both local and global errors are used to define a new mesh is required. An appropriate methodology is the h-type adaptive procedure which must obey the following conditions: (i) the global relative error (r_Ω) must be lower than an imposed value and (ii) the local error indicator (ϕ_i) should be close to unity. The global relative error is defined as

$$r_\Omega^2 = \frac{\sum_{i=1}^{nt} \| e_i \|_{H_1}^2}{\sum_{i=1}^{nt} \| u(\mathbf{x}_i) \|_{H_1}^2} \tag{11}$$

where nt is the number of triangles. According to condition (i), the adaptive procedure establish that $r_\Omega \leq \bar{r}_\Omega$, where $\bar{r}_\Omega$ is the imposed relative error. The local error indicator (ϕ_i) establishes a relationship between the error at triangle Ω_i and the local required error ($\bar{e}_i$). Following this definition, the local indicator is defined as

$$\phi_i = \frac{\| e_i \|_{H_1}}{\| \bar{e}_i \|_{H_1}} \tag{12}$$

The definition of the local required error provides the homogeneous distribution of the error in each mesh triangle. Due to the additive property of the norm (Herbin and Marchand, 2001), the following expression can be used to evaluated the distributed error:

$$\| \bar{e}_i \|_{H_1} = \frac{\bar{r}_\Omega \| u(x_i) \|_{H_1}}{\sqrt{nt}} \tag{13}$$

Notice that, if $\phi_i = 1$, an optimal triangle size is obtained, since the local error has the same magnitude of the local required value. However, $\phi_i < 1$ or $\phi_i > 1$ indicates that further local size modification should be performed. It is acceptable that the local error indicator can be used to define the new size distribution on the mesh, according to the equation:

$$h_i = \frac{h_i^0}{\phi_i} \tag{14}$$

where h_i and h_i^0 are the new and the current size of the triangle Ω_i, respectively.

The complete adaptive solution procedure is presented in Fig. 2 and further information regarding h-type mesh refinement can be found in Zienkiewicz and Zhu (1991) and Bugeda (2000), and it generates information on refinement and derefinement of the mesh. Further information on the adaptive time stepping methodology used in this work can be found in Bixler (1989).

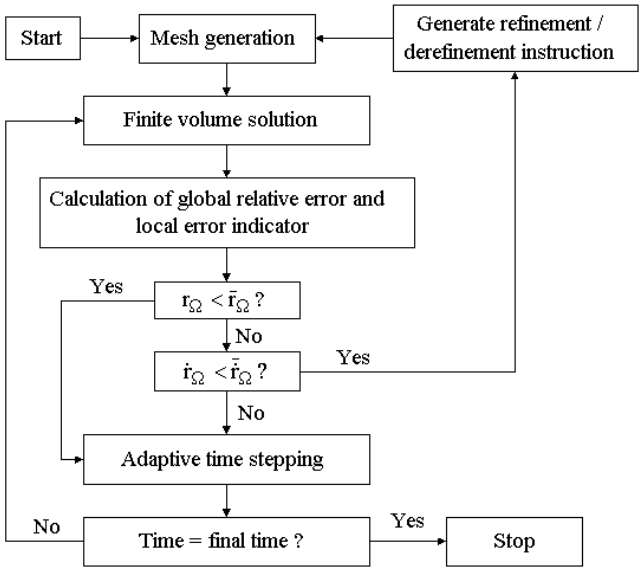

Figure 2. Procedure used for adaptive finite volume solution.

The adaptive procedure stores the new size distribution in the appropriate centroids of the previous mesh. Then, a least-squares method is used to interpolate the triangle size from the centroids to the respective triangle nodes. At the end, a size distribution stored at the nodes of the previous mesh is obtained. This mesh is used as a background mesh by the mesh generator to generate a new one. Starting with an initial tentative mesh the adaptive procedure generates the first adaptive mesh, then the whole procedure is restarted using this new first mesh.

In time-dependent problems, the adaptive procedure should be performed after a set of time steps advances in order to assure that the error is always below the prescribed value. Although this methodology has been used in several finite element-based studies (Lewis et all, 1991), a calculation of the variation of the error with respect to time is preferred

(Oliveira et all,1995). The evaluation of the error rate prevent unnecessary remeshing, i.e. generate a new mesh when the error is decreasing at a reasonable rate for the actual mesh. The error rate ($\dot{r}_\Omega$) is given by

$$\dot{r}_\Omega = \frac{r_\Omega\big|_{t+\Delta t} - r_\Omega\big|_t}{\Delta t} \tag{15}$$

The interpolation of the cell-centered information from one mesh to another is carried out using Taylor series up to the first derivative.

Three test cases, representing generic time-dependent heat transfer problems, are presented in the next sections to evaluate the behavior of the proposed error estimate, the adaptive time stepping and the mesh enhancement. The test cases were selected in a way that the effects of essential, natural and mixed boundary conditions could be evaluated. Also, the selected problems have either exact or analytical solutions, so a comparison between the exact and the estimated error can be performed.

4. Adaptive solution

The first test case consists on a dimensionless parabolic problem with Dirichlet and Neumann boundary conditions. Defining $\Omega =]0, 1[\times]0, 1[$ and t = [0, 0.001], this problem is stated as

$$\frac{\partial u(\mathbf{x}, t)}{\partial t} - \nabla \cdot \nabla u(\mathbf{x}, t) = 0 \tag{16}$$

in which the initial and boundary conditions are depicted in Fig. 3a.

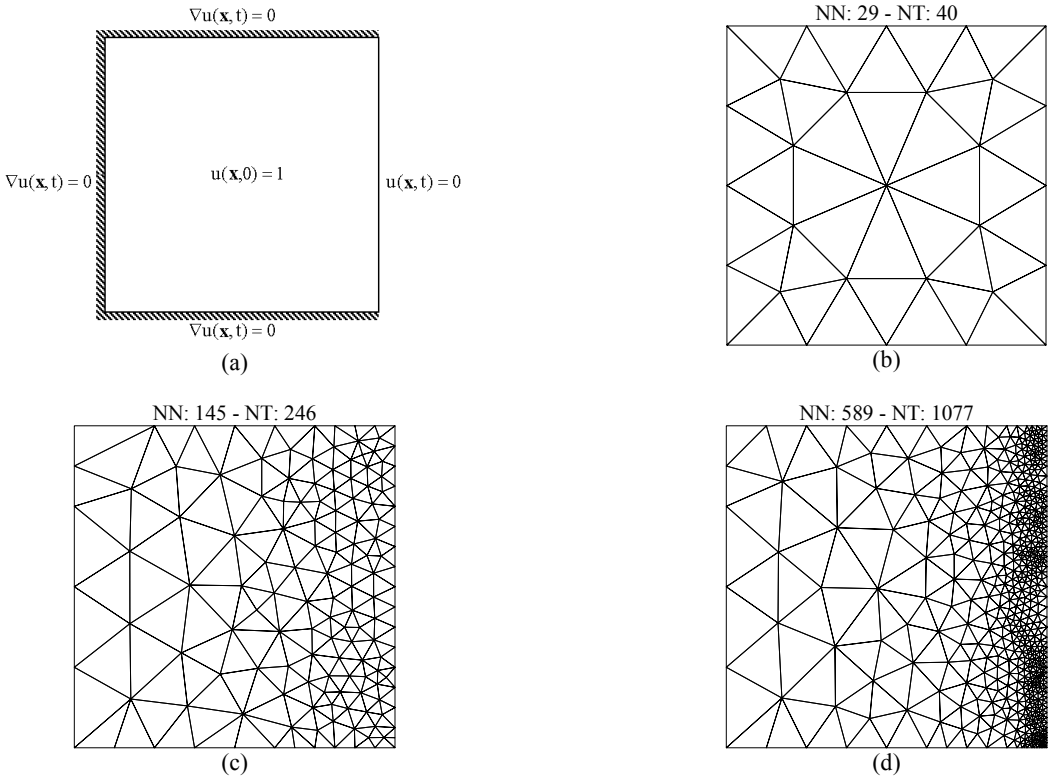

Figure 3. Initial and boundary conditions (a), initial mesh (b), first mesh (c) and final mesh (d) for test case 1.

The solution is started using and arbitrary initial mesh (Fig. 3b), where NN and NT denote the numbers of nodes and triangles, respectively. After the first mesh (Fig. 3c) has been generated, the solution procedure is restarted using this mesh. Both adaptive meshes (Figs. 3c and 3d) are more refined near the right boundary, as expected, since the gradients are steeper in this region. For this test case, the imposed relative error was 5% or $\bar{r}_\Omega = 0.05$, and the initial time step was $\Delta T = 10^{-6}$. The simulation was carried out and the final relative error was 0.0417. Although $\Omega \in \mathbf{IR}^2$, u(**x**,t) varies only in the x direction due to the boundary conditions presented in Fig. 3a. The exact and finite volume solutions for u(**x**,t) at t = 0.001 are presented in Fig. 4.

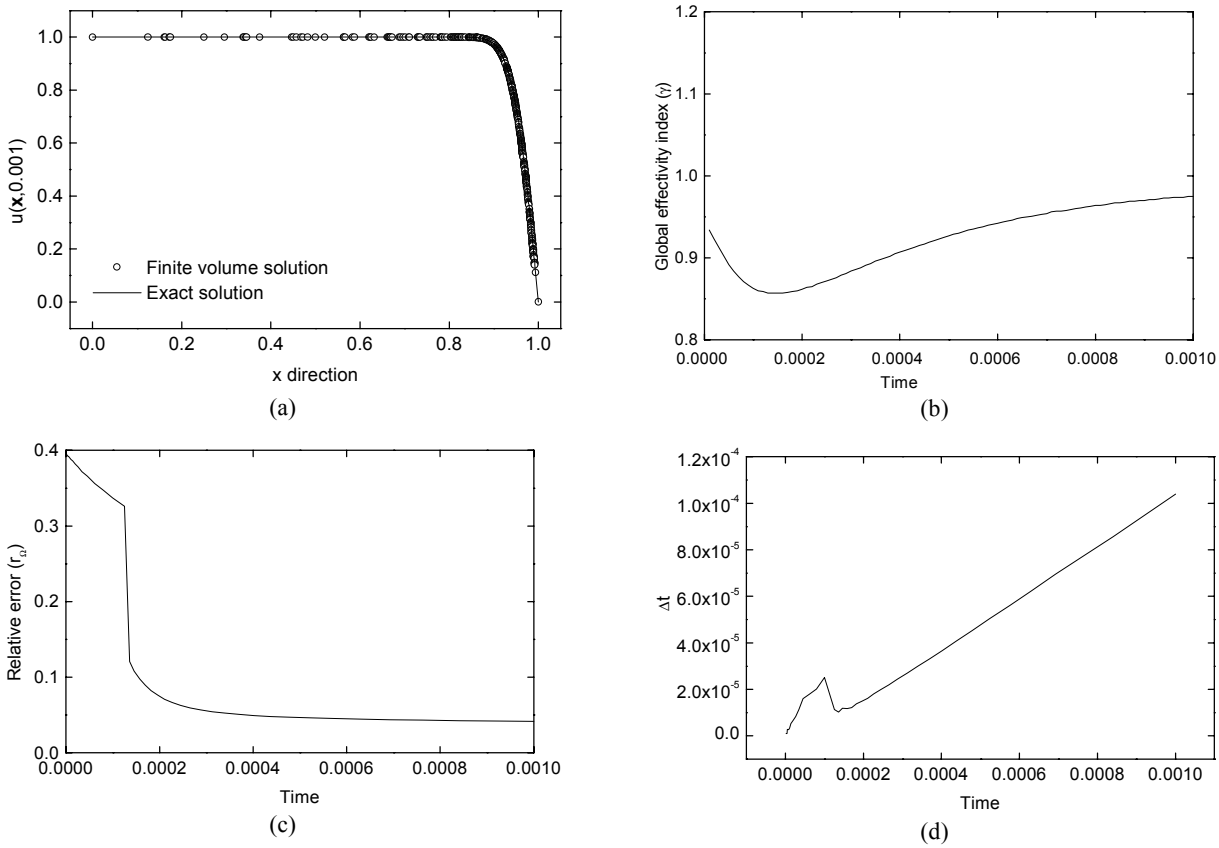

Figure 4. Exact and finite volume solutions at t = 0.001(a), and variation of the global effectivity index (b), relative error (c), and time step size (d) with time for test case 1.

Figure 4a shows that the finite volume solution presented a very good agreement with the exact solution as also presented by the global effectivity index (γ) profile in Fig. 4b. This index is a measure of the accuracy of the estimated error and it is defined as

$$\gamma = \frac{\| e \|}{\| E \|} \tag{17}$$

where || E || and || e || are the exact and the estimated errors, respectively. The value of γ tends to 1 with time and its minimum was γ = 0.867. This behavior of global effectivity index (Fig. 4b) demonstrates the efficiency and reliability of the proposed error estimate. The exact solution for test case 1 is given by Carslaw and Jaeger (1986).

The number of meshes generated in the adaptive procedure depends on the problem, since the gradients vary with time. In this test case only one mesh enhancement was necessary to reach the imposed relative error. The new mesh was generated at $t = 2.52\times10^{-5}$ and the effect of the mesh refinement on the relative error is presented in Fig. 4c. It can be verified that mesh refinement is applied after few time iterations, in spite of the relative error to be higher than the imposed value (5%). This is due to the fact that the proposed adaptive procedure (Fig. 2) checks not only the relative error, but also its variation with respect to time. Thus, if the relative error decreases reasonably with time, no mesh enhancement will be applied. When the relative error tends to be invariant with time, the mesh refinement proceeds in order to reduce this error value.

Figure 4d presents the time step (Δt) variation with time. The slight increase up to $t = 2.52\times10^{-5}$ is due to the continuously decreasing of $\nabla u(\mathbf{x},t)$ with time. The subsequent decrease of Δt at the mesh refinement is due to the interpolation error in the adaptation of the solution from the old to the new mesh. After few iterations the time step increases again as the gradient decreases.

The second test case consists on a convective meat heating. Defining a slab of meat with domain $\Omega =]0,\ 0.2[\ \mathrm{m} \times]0, 0.1[\ \mathrm{m}$ and $t = [0,\ 1800]$s, this problem is stated as

$$\frac{\partial u(\mathbf{x},t)}{\partial t} - \nabla \cdot \alpha \nabla u(\mathbf{x},t) = 0 \tag{18}$$

where $\alpha = 1.875\times10^{-7}$ m^2/s is the thermal conductivity (Kreith and Black, 1980). The meat slab, initially at 10 ºC, is heated by convection (h = 30 W/m^2·s) with surroundings at 160 ºC for 1800 s (or 30 minutes), where h is the heat

transfer coefficient. The upper and the right boundaries exchange heat by convection with the environment and the lower and left boundaries are kept insulated.

The initial mesh is presented in Fig. 5a, and the final mesh is presented in Fig. 5b. This adaptive mesh is more refined near the upper and the right boundaries, as expected, and it was such that there was no need for another refinement.

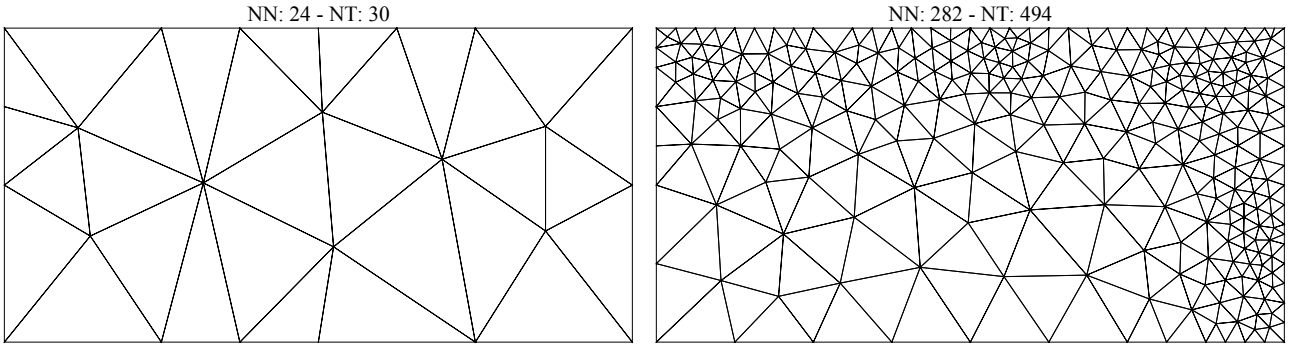

Figure 5. Initial (a) and final meshes (b) for test case 2.

The imposed relative error and the initial time step were 10% and 10^{-3}s, respectively, and the final relative error at the final time was 0.071. The exact and finite volume solutions for u(**x**,t) at t = 1800s are presented in Fig. 6.

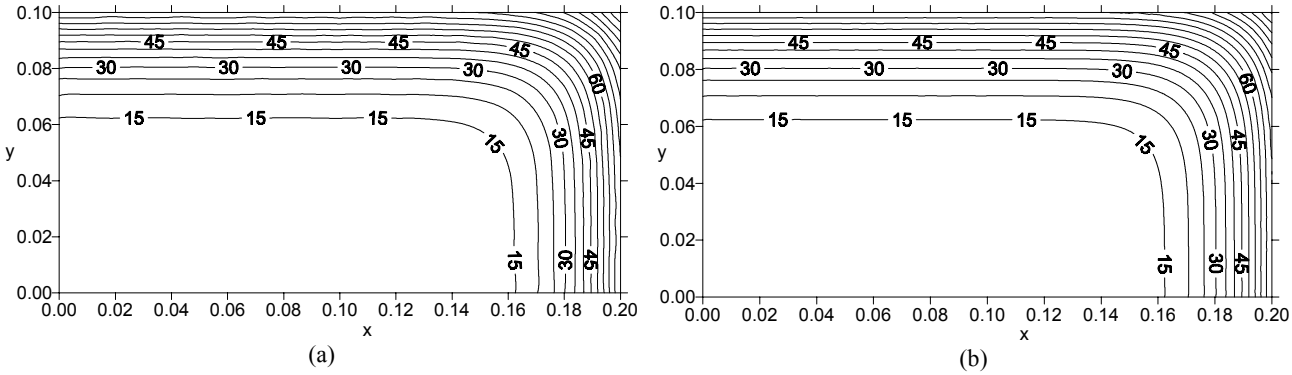

Figure 6. Finite volume (a) and exact (b) solutions at t = 1800 s for test case 2.

Figure 6 shows that the finite volume solution presented a very good agreement with the exact solution. It can be verified that the mesh refinement (Fig. 5b) is concentrated near the upper and right boundary, where the temperature gradients are stepper (Fig. 6). The variation of the relative error and the time step size with time is presented in Fig. 7

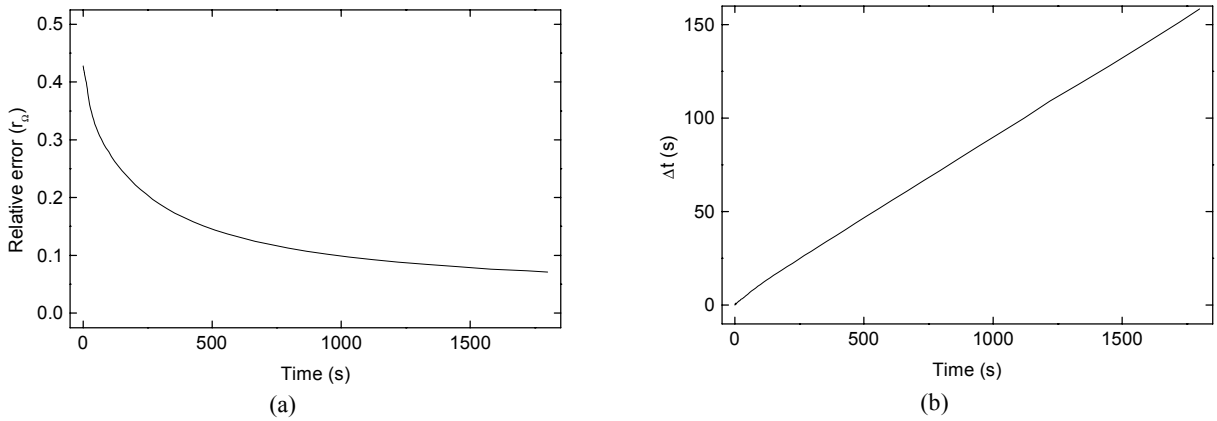

Figure 7. Variation of the relative error (a) and time step size (b) with time for test case 2.

In this test case, the new mesh (Fig. 5b) was generated at t = 2.18 s and its effect on the relative error can not be verified in Fig. 7, because the mesh enhancement took place at the first iteration, since the relative error decreases slower than in test case 1. If the mesh refinement does not occur after a few iterations, the relative error will decrease

continuously up to the final time, but the imposed relative error will not be reached. This situation is eliminated with the proposed methodology, in which not only the relative error is checked, but also the relative error rate. Since there is not a sudden decrease in the relative error, the time step size variation with time (Fig. 7b) increases as the relative error decreases. The global effectivity index variation with time is presented in Fig. 8.

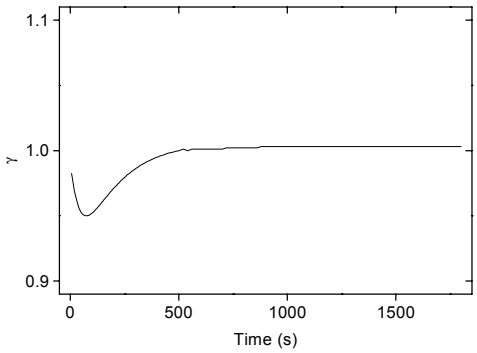

Figure 8. Variation of the global effectivity index with time for test case 2.

The global effectivity index tended to 1 with time, with a minimum value of $\gamma = 0.951$. Thus, it can be observed that the proposed error estimate consists on an efficient and reliable methodology. A comparison between Fig. 4b and Fig. 8 shows a very close behavior of γ since these test cases have similar relative error variation with respect to time. The analytical solution for test case 2 can be found in Carslaw and Jaeger (1986).

The third test case consists on a dimensionless problem with domain $\Omega =]0, 1[\times]0, 1[$ and t = [0, 20]. This problem is stated as

$$\frac{\partial u(\mathbf{x}, t)}{\partial t} - \nabla \cdot \nabla u(\mathbf{x}, t) = f(\mathbf{x}, t) \tag{19a}$$

$$f(\mathbf{x}, t) = xy\left[(1-x)(1-y)\right]^{t+1}(t+1)^3\left[\frac{\ln(1-x)+\ln(1-y)}{t+1} + \frac{2}{(t+1)^2} + \frac{2-2x-xt}{x(1-x)^2} + \frac{2-2y-yt}{y(1-y)^2}\right] \tag{19b}$$

$$u(\mathbf{x},0) = xy(1-x)(1-y) \tag{19c}$$

The Dirichlet boundary condition $u(\mathbf{x},t) = 0$ on whole $\partial\Omega$ was used. The initial mesh used was the same presented in Fig. 5a. Four meshes were generated by the adaptive procedure and they are presented in Figs. 9 and 10.

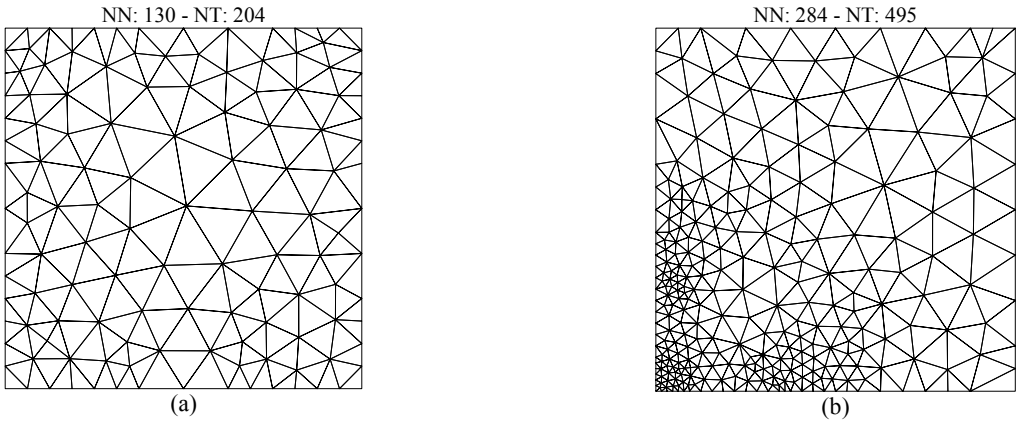

Figure 9. First (a) and second (b) adaptive meshes for test case 3.

The time-dependent source term (Eq. 19b) increases in modulus and moves to the lower-left corner of Ω, so it generates an increasing gradient with time. The imposed relative error and the initial time step were 10% and 10^{-3}s, respectively, and the final relative error at t = 20 was 0.0609. The exact and finite volume solutions for $u(\mathbf{x},t)$ at t = 3.08, t = 8.61 and t = 20.00 are presented in Figs. 11 and 12, respectively.

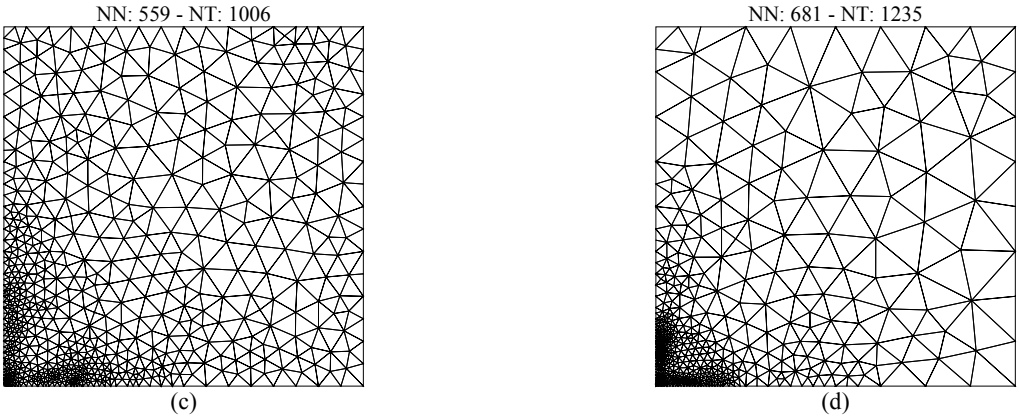

Figure 10. Third (a) and fourth (b) adaptive meshes for test case 3.

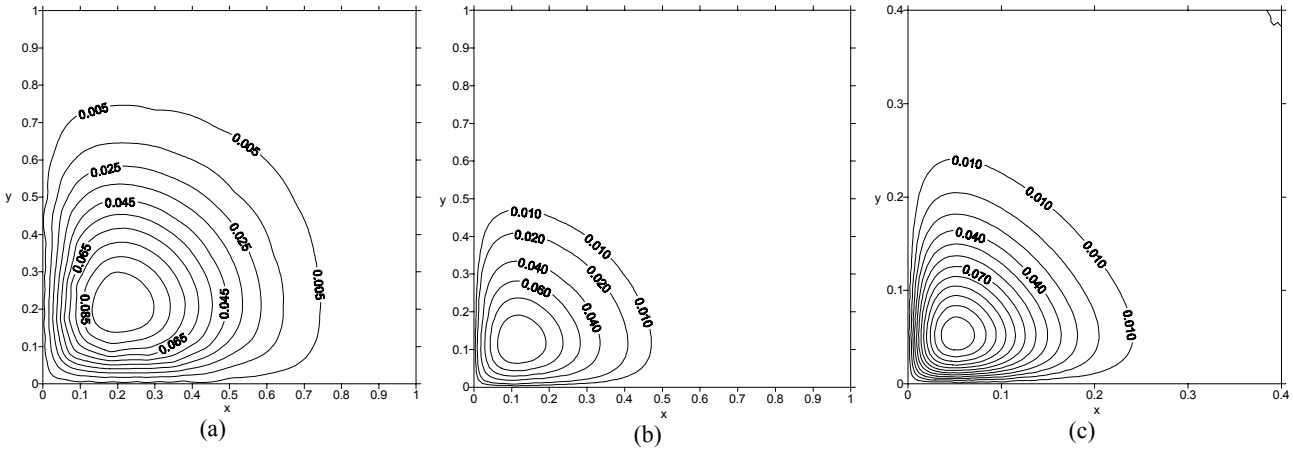

Figure 11. Exact solution at t = 3.08 (a), t = 8.61 (b) and t = 20.00 (c) for test case 3.

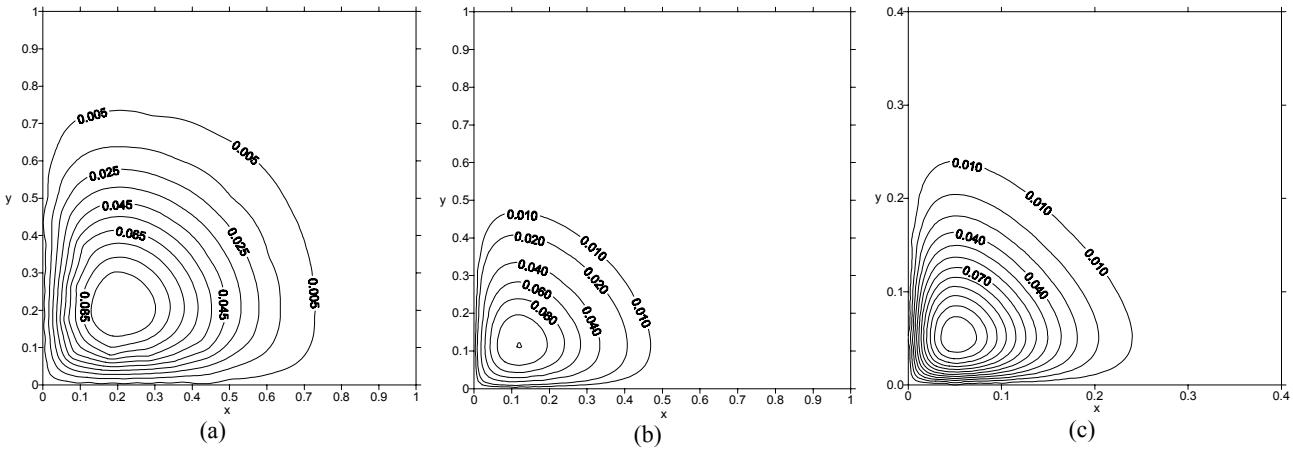

Figure 12. Finite volume solution at t = 3.08 (a), t = 8.61 (b) and t = 20.00 (c) for test case 3.

Figures 11 and 12 show that the finite volume solution presented a very good agreement with the exact solution at three different times. Figures 11c and 12c had their scale changed for clarity. By means of these results, it can be noted that the gradients increases continuously and the mesh refinement (Figs 9 and 10) is applied in order to reduce the increasing local errors. The variation of the relative error and the time step size with time is presented in Fig. 13.

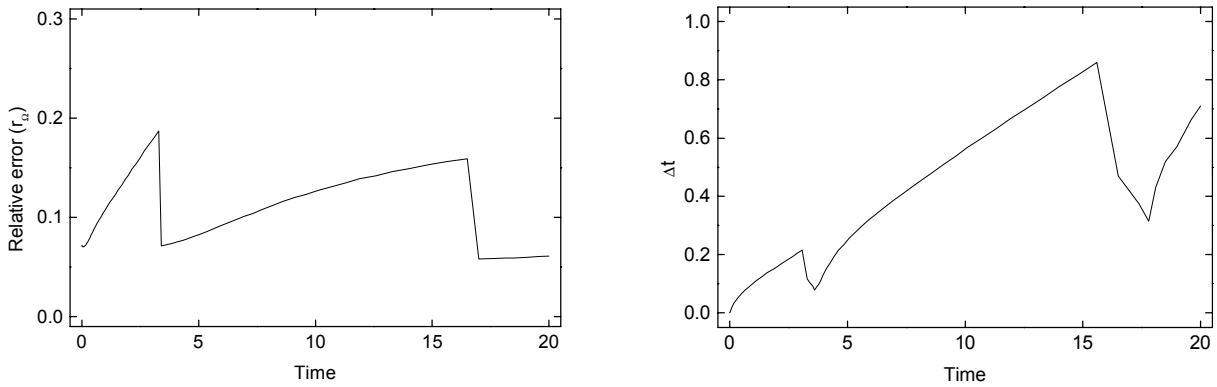

Figure 13. Variation of the relative error (a) and time step size (b) with time for test case 3.

Different from the previous test cases, the relative error increases with time (Fig 13a). The mesh refinement is applied when the relative error overcomes the imposed value (10%). In this test case, the mesh enhancement effect over the relative error and time step size is clearly verified in Figs. 13a and 13b. The global effectivity index variation with time is presented in Fig. 14.

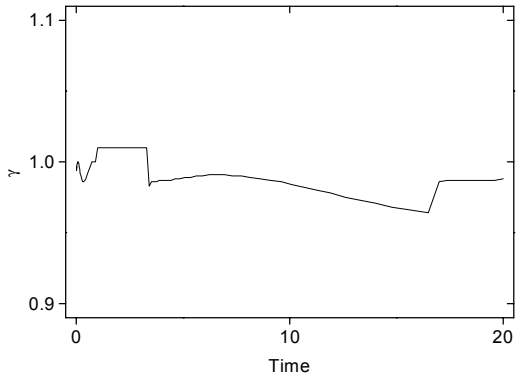

Figure 14. Variation of the global effectivity index with time for test case 3.

Figure 14 shows that the global effectivity index varies closed to 1 with time and its value at t = 20 was $\gamma = 0.987$. It can also be verified that mesh refinement affects the global effectivity, although its minimum was quite closed to 1 (0.964). The sudden deviation from unity is observed only when the mesh refinement occurs. The exact solution for test case 3 is

$$u(\mathbf{x}, t) = xy\left[(1-x)(1-y)\right]^{t+1}(t+1)^2 \tag{20}$$

Typical parabolic heat transfer problems similar to test case 3 are the punctual welding problems, in which a heat source moves in the domain producing localized temperature gradients.

5. Conclusions

In this paper, a simple and reliable error estimate and adaptive procedure were presented for finite volume methods on unstructured triangular meshes. The error estimate formulation is suitable for elliptic and parabolic problems since it allows the establishment of relationship between the error norm and the triangles sizes. Although the energy norm has not been extensively used by the finite volume community, it was shown that this norm is reliable to measure the error, since the finite volume discretization is based on the gradient (i.e. heat flux across the cell faces). The adaptive solution of parabolic problems in this work demonstrated that both the proposed error estimate and adaptive procedure were able to handle boundary conditions of essential, natural and mixed kind. Hence, the proposed methodology could be used to solve problems with high local moving gradients. Further studies will be concerned on alternative methodologies for improving the triangle's size distribution.

6. Acknowledgement

Marcio Arêdes Martins is grateful for the support of the Brazilian government agency CAPES for a scholarship to carry out this study.

7. References

Arminjon, P. and Madrane, A., 1999, "Staggered mixed finite volume/finite element method for Navier-Stokes equations", AIAA J., vol. 37, pp. 1558-1571.

Arbogast, T., Wheeler, M.F. and Yotov, I., 1997, "Mixed finite element for elliptic problems with tensor coefficients as cell-centered finite differences", SIAM J. Num. Anal., vol. 34, pp. 828-852.

Baranger, J., Maitre, J.-F. and Oudin, F., 1996, "Connections between finite volume and mixed finite element methods", Modél. Math. Anal. Numér., vol. 30, pp. 444-465.

Berger, M.J. and Collela, P., 1989, "Local adaptive mesh refinement for shock hydrodynamics", J. Comput. Phys., vol. 82, pp. 64-84.

Bixler, N.E., 1989, "An improved time integrator for finite element analysis", Comm. Appl. Num. Meth., vol. 5, pp. 69-78.

Bugeda, G., 2000, "A comparison between different adaptive remeshing strategies based on different global and local optmality criteria", Proc. European Congress on Computational Methods in Applied Science and Engineering, pp. 1-18, Barcelona.

Carslaw, H.S and Jaeger, J.C, 1986, "Conduction of Heat in Solids", Oxford University Press Inc., London.

Coudière, Y., Vila, J. -P. and Villeudieu, P., 1999, "Convergence rate of a finite volume scheme for a two dimensional convection-diffusion problem", Modél. Math. Anal. Numér., vol. 33, pp. 493-516.

Eymard, R., Gallouët, T. and Herbin, R., 1997, "Finite volume methods" (To appear in Handbook of Numerical Analysis, P.G. Ciarlet, J.L. Lions Editors), Preprint 97-19 of LATP, UMR 6632, Université de Provence, Marseille, Chap. 3.

Feistauer, M., Felcman, J. and Lukacova-Medvidova, M., 1997, "On the convergence of a combined finite volume-finite element method for nonlinear convection-diffusion problems", Numer. Meth. for P.D.E.'s, vol. 13, pp. 163-190.

Frink, N.T., 1994, "Recent progress toward a three-dimensional unstructured Navier-Stokes flow solver", AIAA Paper 94-0061, Reno, Nevada.

Galouët, T. and Herbin, R., 1996, "Finite volume approximation of elliptic problems with irregular data", Finite Volume for Complex Applications, Problems and Perspectives II, pp. 155-162, F. Benkhaldoun, R. Vilsmeier and Hänel eds, Hermes, Paris.

Haselbacher, A., McGuirk, J.J. and Page, G.J., 1999, "Finite volume discretization aspects for viscous flows on mixed unstructured grids", AIAA Journal, vol. 37, pp. 177-184.

Herbin, R., 1995, "An error estimate for a finite volume scheme for a diffusion-convection problem on a triangular mesh," Numer. Meth. P.D.E.'s, vol. 11, pp. 165-173.

Herbin, R. and Marchand, E., 2001, "Finite volume approximation of a class of variational inequalities", IMA J. Num. Anal., vol. 21, pp. 553-585.

Ilinca, C., Trépanier, J.-Y. and Camarero, R., 1995, "Error estimator and adaptive moving grids for the finite volume schemes", AIAA J., vol. 3, no. 11, pp. 2059-2065, 1995.

Ilinca, C., Zhang, X.D., Trépanier, J.-Y. and Romero, R., 2000, "A Comparison of Three Error Estimation Techniques for Finite-Volume Solutions of Compressible Flows", Comput. Meth. App. Mech. Eng., vol. 189, pp. 1277-1294.

Klopfer, G.H. and McRae, D. S., 1983, "Nonlinear truncation error analysis of finite difference schemes for the Euler equations", AIAA J., vol. 21, pp. 487-494.

Kreith, F., and Black, W.Z., 1980, "Basic Heat Transfer", Harper & Row, New York.

Lewis, R.W., Huang, H.C., Usmani, A.S., and Cross, J.T., 1991b, "Finite Element Analysis of Heat Transfer and Flow Problems Using Adaptive Remeshing Including Application to Solidification Problem, Int. J. Numer. Meth. Eng., vol. 32, pp. 767-781.

Oliveira, L.S., Franca, A.S., and Haghughi, K., 1995, "An adaptive approach to finite element modeling of drying problems", Drying Technology, Vol. 13, n. 5-7, pp.1167-1185.

Pan, D. and Cheng, P., 1993, "A second-order upwind finite-volume method for the euler solution on unstructured triangular meshes", Int. J. Num. Meth. Fluids, vol. 16, pp. 1079-1098.

Thompson, M.C. and Ferziger, J.H., 1989, "An adaptive multigrid technique for the incompressible Navier-Stokes equations", J. Comput. Phys., vol. 82, pp. 94-121.

Zhang, X.D., Trépanier, J.-Y. and Camarero, R., 2000, "A posteriori error estimation for finite-volume solutions of hyperbolic conservation laws", Comp. Meth. App. Mech. Eng., vol. 185, no. 1, pp. 1-19.

Zienkiewicz, O. C. and Zhu, J. Z., 1991, "Adaptivity and mesh generation", Int. J. Numer. Meth. Engng., vol. 32, pp. 783-810.